Unexpected universality in static and dynamic avalanches

Yang Liu and Karin A. Dahmen
Department of Physics, University of Illinois at Urbana-Champaign, Urbana, Illinois 61801, USA
(Received 1 March 2009; revised manuscript received 27 April 2009; published 24 June 2009)

We find that some equilibrium systems and their nonequilibrium counterparts actually show the same jerky response or avalanche behavior on many scales in response to slowly changing external conditions. In other words, their static and dynamic avalanches behave statistically the same. This suggests that their critical properties are much more generally applicable than previously assumed. In this case, systems far from equilibrium may be used to predict equilibrium critical behavior and vice versa.

DOI: 10.1103/PhysRevE.79.061124 PACS number(s): 75.10.Nr, 05.40.−a, 64.60.av, 75.60.Ej

Avalanche behavior in diverse dynamical systems has been extensively studied in the past decade [1–4]. In those systems, there are often a large number of metastable states. When pushed by an external driving field, those systems shift from one metastable state to another responding with collective behavior in the form of avalanches. A dynamic avalanche is just the rearrangement of the system configuration, which connects two different metastable states at two slightly different external fields. In experiments, avalanches are often associated with crackling noise as measured in acoustic emission and Barkhausen noise experiments [2,3]. So far, avalanche behavior in equilibrium systems, i.e., static "avalanche," has rarely been studied due to computational complexity. With a static avalanche we refer to a configuration rearrangement connecting two different neighboring ground states at two slightly different external fields.

Generally, equilibrium systems are believed to be completely different from nonequilibrium ones simply because the underlying physics is so different. A natural question arises: Do static and dynamic avalanches have the same critical behavior? Answering this basic question would be crucial to understand whether there are any possible deep connections between equilibrium systems and their nonequilibrium counterparts.

In this paper, we show compelling evidence that static and dynamic avalanches have the same critical behavior in the zero-temperature random-field Ising model (zt-RFIM). This particular model is chosen for two reasons. First, there is a related highly controversial question in this model, i.e., whether the equilibrium and nonequilibrium disorder-induced phase transitions belong to the same universality class. Second, both static and dynamic avalanches can be clearly identified and calculated within this model. We find that all tested universal scaling functions and corresponding critical exponents coincide for static and dynamic avalanches. Our findings indicate that generally equilibrium systems and their nonequilibrium counterparts may have deep connections [5,6].

As a prototypical model for disordered magnets, the RFIM has been intensely studied [7]. Its Hamiltonian is given by $\mathcal{H}=-J\Sigma_{\langle i,j\rangle}s_i s_j-\Sigma_i(H+h_i)s_i$ where the Ising spins $s_i=\pm 1$ sit on a d-dimensional hypercubic lattice with periodic boundary conditions. The spins interact ferromagnetically with their nearest neighbors with strength J and experience a uniform external field H and a quenched local random field h_i. Usually, the local fields are chosen from a Gaussian distribution $\rho(h)$ with mean 0 and standard deviation R. R is called the disorder parameter. In equilibrium, it is generally believed that in $d>2$ the transition between the ordered (ferromagnetic) and disordered (paramagnetic) phases is continuous and controlled by a stable zero-temperature fixed point [8]. Therefore, one can set temperature $T=0$ and tune disorder R to study the equilibrium disorder-induced phase transition (DIPT) undergone by the ground-state properties. In nonequilibrium, the zt-RFIM has been very successful in explaining dynamic avalanches and crackling noise observed in magnets [9–11]. The key result is that there is a nonequilibrium DIPT associated with the hysteretic behavior. Based on the similarities of some critical exponents, it has been conjectured that the equilibrium and nonequilibrium DIPT may belong to the same universality class. But this has been highly controversial due to the lack of compelling evidence [5,6,12,13]. Comparing the critical behavior of static and dynamic avalanches is important and necessary to answer this question.

An avalanche in the RFIM refers to the flip of neighboring spins during the magnetization process corresponding to a jump in the magnetization curve $M(H)$. To identify avalanches, we increase the external field H from $-\infty$ to ∞ adiabatically slowly; i.e., H is kept constant during the propagation of an avalanche. Then, a static (dynamic) avalanche connects two *nearest* ground (metastable) states along the equilibrium (nonequilibrium) $M(H)$ curve at zero temperature. In equilibrium, the ground-state problem of the RFIM can be mapped onto the min-cut/max-flow problem of a network and solved via the so-called push-relabel algorithm [14,15]. An efficient linear interpolation scheme is then used to find steps by narrowing down the H range where static avalanches occur [16]. In nonequilibrium, we use the single-spin-flip dynamics to calculate the metastable state: each spin flips deterministically when its effective local field $h_i^{\text{eff}}=J\Sigma_j s_j+h_i+H$ changes sign [9,11]. Due to the nearest-neighbor interaction, a flipped spin will push a neighbor to flip, which in turn might push another neighbor, and so on, thereby generating a dynamic avalanche.

To study whether the shape of the random-field distribution would affect the avalanche behavior, we consider four different types of $\rho(h)$'s: (1) Gaussian: $\rho_{\text{G}}(h)=\frac{1}{\sqrt{2\pi}R}\exp(-\frac{h^2}{2R^2})$; (2) Lorentzian: $\rho_{\text{L}}(h)=\frac{1}{2\pi}\frac{R}{h^2+(R/2)^2}$; (3) parabolic: $\rho_{\text{P}}(h)=\frac{R^2-h^2}{4R^3/3}$ for $h\in[-R,R]$ and 0 else; (4) uniform: $\rho_{\text{U}}(h)=\frac{1}{2R}$ for $h\in[-R,R]$ and 0 else. In all cases, $\rho(h)$ is

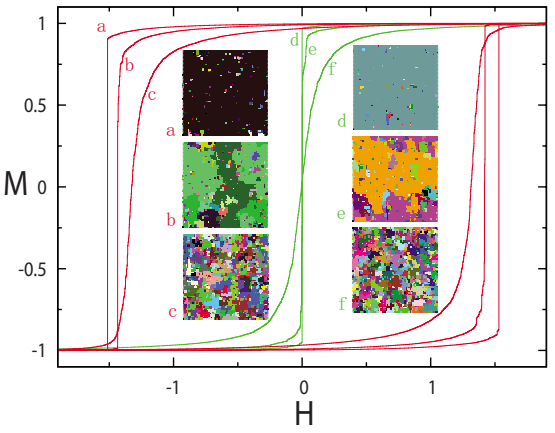

FIG. 1. (Color online) Disorder-dependent avalanche behavior in RFIM. Main panel: magnetization curves in equilibrium (d,e,f) and nonequilibrium (a,b,c) below, near, and above the critical disorder R_c. Insets: cross sections of three-dimensional (3D) systems showing all the avalanches (denoted by different colors) occurring during those magnetization processes. The calculation is done on 3D Gaussian zt-RFIM with system size 64^3. Nonequilibrium: (a) $R=2.0$, (b) $R=2.224$, and (c) $R=2.6$. Equilibrium: (d) $R=2.25$, (e) $R=2.45$, and (f) $R=2.9$. Note that $R_c^{neq}=2.16\pm0.03$ and $R_c^{eq}=2.28\pm0.01$ for 3D Gaussian RFIM [11,17].

symmetric around $h=0$ and the generalized "width" R will be called the disorder parameter.

Figure 1 shows the $M(H)$ curves and corresponding avalanches occurring during the magnetization processes at different disorders in both equilibrium [(d)–(f)] and nonequilibrium [(a)–(c)]. For $R<R_c$ [(a) and (d)], most spins tend to flip collectively in a system spanning avalanche seen as a macroscopic jump in the magnetization curve. For $R>R_c$ [(c) and (f)], spins tend to flip individually and result in many microscopic avalanches and a macroscopically smooth magnetization curve. For $R\sim R_c$ [(b) and (e)], jumps (avalanches) of all sizes are seen in the magnetization curve. Qualitatively, we find that static and dynamic avalanches show similar disorder-dependent behavior.

To quantitatively study the similarity of static and dynamic avalanches, we first study the avalanche size distribution integrated over the external field [11]. Near the critical disorder R_c, its scaling form can be written as

$$D_{\rm int}(S,R) \sim S^{-(\tau+\sigma\beta\delta)}\overline{\mathcal{D}}_{\pm}^{\rm int}(S^{\sigma}|r|), \qquad (1)$$

where S is the avalanche size, i.e., the number of spins participating in an avalanche, $\pm$ refers to the sign of the reduced disorder $r=(R_c-R)/R$, σ gives the scaling of the largest avalanche size $S_{\max}\sim|r|^{-1/\sigma}$, and β and δ give the singularities of $M(H)$ near the critical point (H_c,R_c). Here, the critical field H_c is defined to be the field where the slope of $M(H)$ goes to ∞. In nonequilibrium, $D_{\rm int}(S,R)$ for Gaussian $\rho(h)$ has been studied extensively. The critical exponents $(\tau+\sigma\beta\delta)=2.03\pm0.03$, $\sigma=0.24\pm0.02$, and the universal scaling function $\overline{\mathcal{D}}_{-}^{\rm int}(X)=e^{-0.789X^{1/\sigma}}(0.021+0.002X+0.531X^2-0.266X^3+0.261X^4)$ were obtained from scaling collapses of $D_{\rm int}(S,R)$ at different disorders [11].

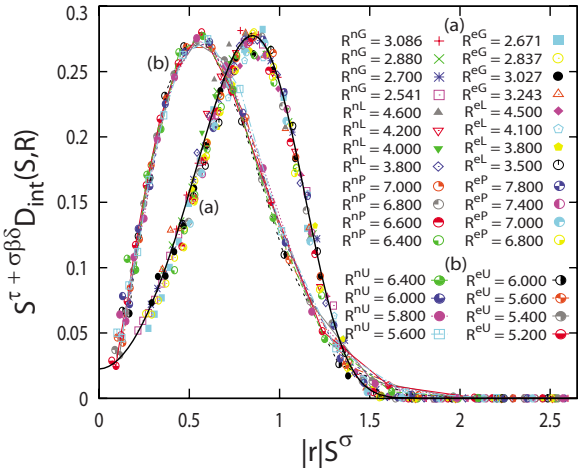

FIG. 2. (Color online) Scaling functions of integrated avalanche size distributions. The original $D_{\rm int}(S,R)$ curves for static and dynamic avalanches at different disorders and different $\rho(h)$'s are calculated in 3D with system size 64^3 and are averaged up to 100 initial random-field configurations. In the legend, the subscripts stand for equilibrium (e) or nonequilibrium (n) and the type of $\rho(h)$: Gaussian (g), Lorentzian (l), parabolic (p), and uniform (u). (a) For Gaussian, Lorentzian, and parabolic $\rho(h)$'s, using critical exponents $(\tau+\sigma\beta\delta)=2.03$ and $\sigma=0.24$, 24 curves collapse onto each other, up to nonuniversal critical disorders ($R_c^{nG}=2.16$, $R_c^{eG}=2.29$; $R_c^{nL}=1.92$, $R_c^{eL}=2.08$; $R_c^{nP}=4.84$, $R_c^{eP}=5.0$) and overall scale factors. The thick black curve through the collapse is the universal scaling function $\overline{\mathcal{D}}_{-}^{\rm int}(X)$ of nonequilibrium Gaussian RFIM [11]. (b) For uniform $\rho(h)$, eight curves collapse onto each other, up to nonuniversal critical disorders ($R_c^{nU}=4.64$, $R_c^{eU}=4.46$) and overall scale factors. The collapse yields critical disorders $(\tau+\sigma\beta\delta)=2.08\pm0.02$ and $\sigma=0.52\pm0.03$. Both the critical exponents and the scaling function are different from those of the Gaussian $\rho(h)$.

Figure 2(a) shows that for Gaussian, Lorentzian, and parabolic $\rho(h)$'s, and for both static and dynamic avalanches at different disorders, with the same pair of critical exponents: $(\tau+\sigma\beta\delta)=2.03$ and $\sigma=0.24$, 24 $D_{\rm int}(S,R)$ curves collapse onto a single one. The universality that the three different $\rho(h)$'s show the same avalanche behavior is not a surprise at all. A renormalization group (RG) analysis has shown that, at least in nonequilibrium, what matters is just $\rho''(0)$, i.e., the second derivative of $\rho(h)$ at $h=0$ [10]. It is easy to check that Gaussian, Lorentzian, and parabolic $\rho(h)$'s all have $\rho''(0)\sim-R^3$. Therefore their universal behaviors agree, as expected. Figure 2(b) shows that for uniform $\rho(h)$, for both static and dynamic avalanches at different disorders, eight $D_{\rm int}(S,R)$ curves collapse onto a single one, with critical exponents: $(\tau+\sigma\beta\delta)=2.08\pm0.02$ and $\sigma=0.52\pm0.03$. Note that: (1) The critical exponents, especially σ, are significantly different from those of the above three kinds of $\rho(h)$'s. (2) The scaling function has a significantly different shape from that observed in Fig. 2(a). These two findings are consistent with the RG analysis mentioned above because for a uniform $\rho(h)$, $\rho''(0)=0$ is independent of R and is qualitatively different from the other three distributions.

The most surprising result about Fig. 2 is that the critical exponents and scaling functions for static and dynamic avalanches match for any $\rho(h)$. This strongly indicates that the

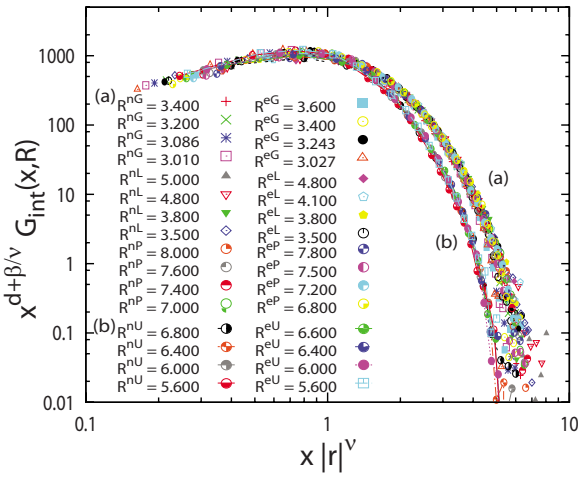

FIG. 3. (Color online) Scaling functions of integrated avalanche correlation function. The original $G_{\rm int}(x,R)$ curves for static and dynamic avalanches at different disorders and different $\rho(h)$'s are calculated in 3D with system size 64^3 and are averaged up to 100 initial random-field configurations. (a) For Gaussian, Lorentzian, and parabolic $\rho(h)$'s, 24 curves collapse onto each other, using $d+\beta/\nu=3.07$ and $\nu=1.37$ [11]. (b) For uniform $\rho(h)$, eight curves collapse onto each other with $d+\beta/\nu=3.0\pm0.3$ and $\nu=0.8\pm0.2$. Note that those collapses are up to the same critical disorders as used in Fig. 2.

equilibrium and nonequilibrium RFIM behave the same near their corresponding critical points.

To check whether this is just a coincidence, we make another independent test by studying the avalanche correlation function, which measures the probability that a distance x between any two flipping spins occurs in the same avalanche [11]. Near the critical disorder R_c, the scaling form of the avalanche correlation function integrated over H can be written as

$$G_{\rm int}(x,R) \sim \frac{1}{x^{d+\beta/\nu}} \overline{\mathcal{G}}_{\pm}(x|r|^{\nu}), \tag{2}$$

with ν the correlation length exponent and d the dimension [10]. In nonequilibrium, the quantity $G_{\rm int}(x,R)$ for the Gaussian $\rho(h)$ has been studied extensively, where $d+\beta/\nu=3.07\pm0.30$ and $\nu=1.37\pm0.18$ were obtained from scaling collapses of $G_{\rm int}(x,R)$ at different disorders [11]. Here, in Fig. 3(a), we show that for Gaussian, Lorentzian, and parabolic $\rho(h)$'s, and for both static and dynamic avalanches at different disorders, with the same pair of critical exponents: $d+\beta/\nu=3.07$ and $\nu=1.37$, 24 $G_{\rm int}(x,R)$ curves collapse onto a single one. Figure 3(b) shows that for uniform $\rho(h)$ and for both static and dynamic avalanches at different disorders, eight $G_{\rm int}(x,R)$ curves collapse onto a single one, with critical exponents: $d+\beta/\nu=3.0\pm0.3$ and $\nu=0.8\pm0.2$. On one hand, both the critical exponents and the scaling function for the uniform $\rho(h)$ are different from those of the Gaussian $\rho(h)$. On the other hand, both the critical exponents and scaling functions for static and dynamic avalanches match for any $\rho(h)$. These results are completely consistent with what we found in avalanche size distributions.

Moreover, in a separate work, for the Gaussian $\rho(h)$, we have shown that static and dynamic avalanches have surprisingly similar spatial structures with the same fractal dimensions, anisotropy measures, and associated universal scaling functions [18]. More interestingly, we notice that the equilibrium and nonequilibrium DIPTs themselves show surprising similarity: (1) they share the same *no-passing rule*: at $T=0$, flipped spins can never flip back as the magnetic field H is swept monotonically [9,19]. (2) In mean-field theory, they have the same thermodynamic critical exponents [9,20], the same avalanche critical exponents [18], and the same exponent relations [10]. (3) RG calculations show that the $6-\epsilon$ expansion for the nonequilibrium critical exponents maps to all orders in ϵ onto the controversial equilibrium ones: the temperature dependence is irrelevant in the equilibrium RFIM and the time dependence is irrelevant in the zero-temperature nonequilibrium RFIM leaving us with the same starting point for the calculation in both cases [10]. All these evidences in favor of universality corroborate our findings here.

To discuss the effect of dynamics on the critical behavior of avalanches, a general k-spin-flip dynamics (with $k=1,2,\ldots,\infty$) has been introduced [6]. It is defined such that all the states connected by avalanches are k-spin-flip metastable states whose energy cannot be lowered by the flip of any subset of $1,2,\ldots,k$ spins [6,21]. The case $k=1$ just corresponds to the single-spin-flip dynamics used in our nonequilibrium calculations. The case $k=\infty$ corresponds to the ground-state evolution dynamics in our equilibrium calculations. It has been found that the change in dynamics from $k=1$ to $k=2$ will not alter the critical behavior of the dynamic avalanches [22]. Together with our finding, i.e., $k=1$ and $k=\infty$ give the same avalanche behavior, we suggest that avalanches associated with the whole series of k-spin-flip dynamics (with $k=1,2,\ldots,\infty$) would have the same critical behavior. The k-spin-flip dynamics is quite general but it definitely cannot encompass all kinds of dynamics, e.g., the demagnetization dynamics associated with the demagnetization curve, which is obtained by applying an oscillating ex-

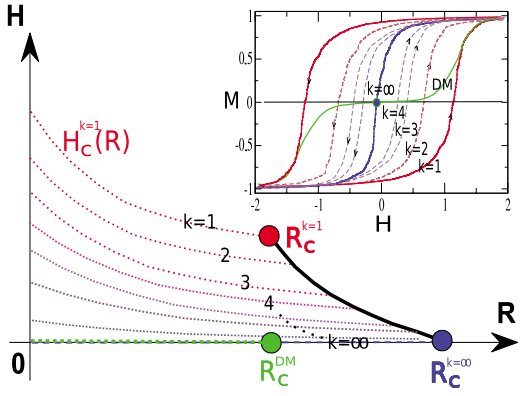

FIG. 4. (Color online) Schematic phase diagram of zt-RFIM with k-spin-flip dynamics and demagnetization dynamics. Dashed lines stand for the first-order phase transitions occurring at the critical field H_c. Note that for both demagnetization dynamics and ground-state evolution ($k=\infty$), $H_c=0$ due to symmetry. (Inset) Schematic $M(H)$ curves associated with different dynamics.

ternal field with very slowly decreasing amplitude. Previous studies for Gaussian $\rho(h)$ showed that there are two very interesting results. First, the avalanches associated with the demagnetization curve are found (within numerical error bars) to display the same critical exponents and scaling functions as the avalanches associated with the saturation hysteresis loop (with $k=1$) [23]. Second, the demagnetized state and ground state show similarity near their corresponding critical disorders: the critical exponents and scaling function associated with the $M(R)$ curve coincide [13].

Considering all the findings, we suggest that all the different dynamics yield the same scaling behavior of avalanches—an unexpected universality, see Fig. 4. It would be very interesting to numerically test this universality in other disordered systems, especially for those systems with frustrations where the no-passing rule is broken. We suspect that a necessary condition for equilibrium and nonequilibrium critical behavior to scale in the same way is that the scaling behavior is dominated in both cases by a zero-temperature fixed point [24]. For example, for the random-bond Ising model, which has a nontrivial finite-temperature fixed point [25], the equilibrium and nonequilibrium critical behavior are different [10].

We thank James P. Sethna, A. Alan Middleton, Yoshitsugu Oono, Daniel S. Fisher, Gil Refael, Andrei A. Fedorenko, Charles M. Newman, and Daniel L. Stein for valuable discussions. We acknowledge the support of NSF Grant No. DMR 03-14279 and NSF Grant No. DMR 03-25939 ITR (Materials Computation Center).

[1] J. P. Sethna, K. A. Dahmen, and C. R. Myers, Nature (London) **410**, 242 (2001).
[2] G. Durin and S. Zapperi, in *The Science of Hysteresis*, edited by G. Bertotti and I. Mayergoyz (Academic Press, New York, 2005).
[3] E. Vives, J. Ortín, L. Mañosa, I. Ràfols, R. Pérez-Magrané, and A. Planes, Phys. Rev. Lett. **72**, 1694 (1994).
[4] S. Field, J. Witt, F. Nori, and X. Ling, Phys. Rev. Lett. **74**, 1206 (1995).
[5] A. Maritan, M. Cieplak, M. R. Swift, and J. R. Banavar, Phys. Rev. Lett. **72**, 946 (1994).
[6] F. J. Pérez-Reche and E. Vives, Phys. Rev. B **70**, 214422 (2004).
[7] D. P. Belanger and T. Nattermann, in *Spin Glasses and Random Fields*, edited by A. P. Young (World Scientific, Singapore, 1998).
[8] D. S. Fisher, Phys. Rev. Lett. **56**, 416 (1986).
[9] J. P. Sethna, K. A. Dahmen, S. Kartha, J. A. Krumhansl, B. W. Roberts, and J. D. Shore, Phys. Rev. Lett. **70**, 3347 (1993).
[10] K. A. Dahmen and J. P. Sethna, Phys. Rev. B **53**, 14872 (1996).
[11] O. Perković, K. A. Dahmen, and J. P. Sethna, Phys. Rev. B **59**, 6106 (1999).
[12] J. P. Sethna, K. A. Dahmen, S. Kartha, J. A. Krumhansl, O. Perković, B. W. Roberts, and J. D. Shore, Phys. Rev. Lett. **72**, 947 (1994).
[13] F. Colaiori, M. J. Alava, G. Durin, A. Magni, and S. Zapperi, Phys. Rev. Lett. **92**, 257203 (2004).
[14] A. A. Middleton and D. S. Fisher, Phys. Rev. B **65**, 134411 (2002).
[15] I. Dukovski and J. Machta, Phys. Rev. B **67**, 014413 (2003).
[16] C. Frontera, J. Goicoechea, J. Ortín, and E. Vives, J. Comput. Phys. **160**, 117 (2000).
[17] A. K. Hartmann and A. P. Young, Phys. Rev. B **64**, 214419 (2001).
[18] Y. Liu and K. A. Dahmen, e-print arXiv:cond-mat/0609609.
[19] Y. Liu and K. A. Dahmen, Phys. Rev. E **76**, 031106 (2007).
[20] T. Schneider and E. Pytte, Phys. Rev. B **15**, 1519 (1977).
[21] C. M. Newman and D. L. Stein, Phys. Rev. E **60**, 5244 (1999).
[22] E. Vives, M. L. Rosinberg, and G. Tarjus, Phys. Rev. B **71**, 134424 (2005).
[23] J. H. Carpenter and K. A. Dahmen, Phys. Rev. B **67**, 020412(R) (2003).
[24] D. S. Fisher (private communication).
[25] K. Hukushima, J. Phys. Soc. Jpn. **69**, 631 (2000).